

Potential sputtering of proton from hydrogen-terminated Si(100) surfaces induced with slow highly charged ions

K. Kuroki,^{a)} N. Okabayashi,^{b)} H. Torii, K. Komaki, and Y. Yamazaki^{b)}

Institute of Physics, Graduate School of Arts and Sciences, University of Tokyo, 3-8-1 Komaba, Meguro, Tokyo 153-8902, Japan

(Received 26 July 2002; accepted 17 September 2002)

A potential sputtering mechanism of hydrogen has been studied for impact of slow highly charged Xe^{q+} ions (<5 keV, $q=4-12$) on well-defined H-terminated Si(100) surfaces. It was found that the sputtering yields of protons are proportional to q^γ ($\gamma\sim 5$), independent of the surface condition, that is, for both Si(100) 2×1 -H surface and Si(100) 1×1 -H surface. The yield for Si(100) 1×1 -H surface was ten times larger than that for Si(100) 2×1 -H surface, although the H coverage of the former is only twice the latter. Surface roughness is found to be the key parameter to vary the yield, and also to influence the energy distribution of sputtered protons. These findings are consistently explained with a pair-wise bond-breaking model induced by a double electron capture, where the classical over barrier process plays an essential role. © 2002 American Institute of Physics. [DOI: 10.1063/1.1520335]

In the last two decades, interactions of slow highly charged ions (HCIs) with various surfaces have been extensively studied because of the exotic nature of the collision dynamics and possible applications to high-sensitivity surface analysis and surface modification.¹⁻⁸ When a slow HCI bombards a solid surface, atoms and molecules on the surface are emitted as neutral and charged particles due to multiple electron transfer and potential energy deposition, which is called potential sputtering. In this case, the kinetic energy of the incident HCI does not play any important role, and can be made small enough so that the radiation damage to the target substrate is negligible. This is compared with kinetic sputtering, which is induced through a kinetic energy transfer from energetic ions. Although kinetic sputtering has been adopted as one of the most popular techniques of surface elemental analysis, radiation damage to the substrate is unavoidable, and could also cause serious problems to the material properties. In this respect, potential sputtering with slow HCIs has two extreme advantages: high sensitivity and low damage, which are usually incompatible.

Proton sputtering induced with slow HCIs has been studied for untreated surfaces (i.e., surfaces covered by water and hydrocarbons), which revealed that the proton yields drastically increase as a function of the charge state q of the HCI [proportional to q^γ ($\gamma\sim 5$)].⁸⁻¹⁰ Similar findings were also reported for higher energy HCIs, where the q -dependence was a bit weaker than the above (e.g., $\gamma\sim 3$ for 18 keV Ar^{q+} ,¹¹ and $\gamma\sim 4$ for 4.8 keV Ar^{q+}).⁹ Such a strong q -dependence in proton sputtering was explained with a pair-wise potential sputtering mechanism based on the classical over barrier model.¹² In contrast to these findings, the sputtering of insulator material is found to be proportional to the potential energy of the incident HCIs, which is interpreted as defect-mediated desorption, where the defects were produced

by localization of electronic excitations via strong electron-phonon coupling.¹³

In the present letter, proton sputtering phenomena were studied for well-defined H-terminated Si(100) surfaces, such as Si(100) 2×1 -H, Si(100) 3×1 -H, and Si(100) 1×1 -H bombarded by Xe^{q+} ($q=4\sim 12, E=2\sim 5$ keV), which allowed a quantitative study of proton sputtering induced with slow HCIs. An n -type Si(100) sample, used as a target, was chemically cleaned by repeated $\text{NH}_4\text{OH}:\text{H}_2\text{O}_2:\text{H}_2\text{O}$ (1:1:5) and $\text{HF}:\text{H}_2\text{O}$ (1:20) treatments. To obtain the reconstructed Si(100) 2×1 clean surface, the sample was heated to 1200 K for 2 min under UHV conditions with a ceramic heater on a sample holder. The base pressure of the collision chamber was 3×10^{-10} Torr, which became $\sim 1\times 10^{-9}$ Torr during the sample heating. The Si(100) 2×1 -H surface was obtained by exposing the clean Si(100) 2×1 surface to atomic hydrogen, keeping the substrate temperature at 600 K until the coverage saturated. The Si(100) 3×1 -H and Si(100) 1×1 -H surfaces were prepared by exposing the Si(100) 2×1 -H surface to atomic hydrogen at 400 K and at room temperature, respectively. The atomic hydrogen was produced by a hot tungsten filament. The procedure to prepare the Si(100) 3×1 -H and Si(100) 1×1 -H surfaces via the Si(100) 2×1 -H surface was found to be quite important to obtain stable data for proton yields, because the clean Si(100) 2×1 surface is quite active and unstable against a tiny amount of water molecules. Pulsed HCI beams were used to sort out the mass of the secondary ions with the time of flight (TOF) technique. The Si crystal sample was positively biased to accelerate secondary ions toward a two-dimensional position sensitive detector located 14 cm from the target. The details of the experimental setup are given elsewhere.^{14,15}

Figure 1 shows an example of the TOF spectrum of secondary ions sputtered from a Si(100) 1×1 -H surface with 2.25 keV Xe^{6+} ion impact, which consisted of proton, Si^+ and Si_2OH_n^+ ($n=0\sim 2$) ions. The Si^+ peak has a tail to

^{a)}NRIPS, 6-3-1 Kashiwanoha, Kashiwa, Chiba 277-0882, Japan; electronic mail: kuroki@nrips.go.jp

^{b)}RIKEN, 2-1 Hirosawa, Wako, Saitama 351-0198, Japan.

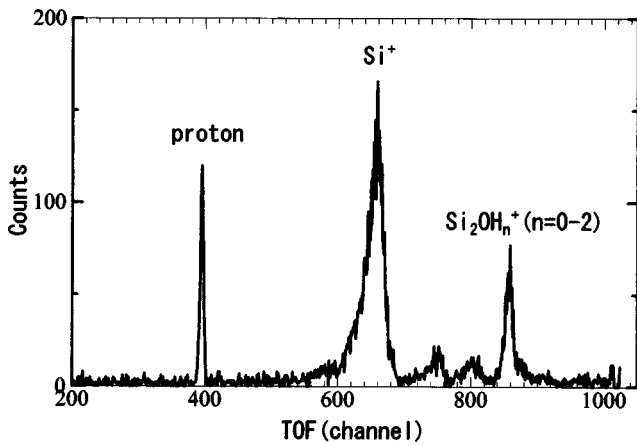


FIG. 1. TOF spectrum of secondary ions sputtered from a Si(100)1×1-H surface with 2.25 keV Xe⁶⁺. The Si target was biased to 325 V.

shorter TOF side, which corresponds to energetic Si⁺ emission induced by kinetic sputtering.

Figure 2 shows the sputtering yields of proton from the Si(100)2×1-H and Si(100)1×1-H surfaces with Xe^{q+} as a function of *q*. As a reference, Si⁺ yields from the same surfaces are also displayed. The dashed lines show *q*⁵ dependence, which more or less reproduce the observed *q*-dependences for both Si(100)2×1-H and Si(100)1×1-H surfaces. As discussed in the introductory section, a similar strong *q* dependence was observed for untreated surfaces,⁹⁻¹¹ which strongly indicates that the principal mechanism of the proton sputtering with slow HCIs does not depend on details of surface conditions. On the other hand, the Si⁺ ion yields were 2.3×10⁻³ and 8×10⁻⁴ for Si(100)1×1-H and 2×1-H surfaces, respectively, and stays constant over the charge states studied. Considering that the total sputtering yield of Si for 3 keV Xe⁺ is about 1.5 atoms/ion,¹⁶ the charged fraction is ~0.1% of the total sputtering yield. It is noted that the sum of Si⁺ and proton yields was almost constant for *q* ≤ 8, and then increased as a function of *q* for *q* ≥ 9, which is qualitatively consistent with the observation for 20 keV Ar^{q+} (1 < *q* < 9) bombardments on a clean amorphized Si(100) surface.¹⁷

Figure 3 shows the sputtering yields of proton and Si⁺ ions from the Si(100)2×1-H surface with 4 keV Xe⁸⁺ im-

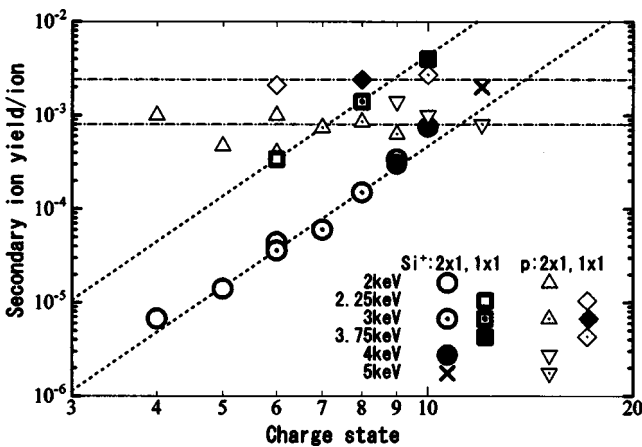


FIG. 2. Sputtering yields of proton and Si⁺ from Si(100)2×1-H and Si(100)1×1-H surfaces as a function of *q*. The dashed lines show *q*⁵ dependence. The energy values are for primary Xe^{q+} ions.

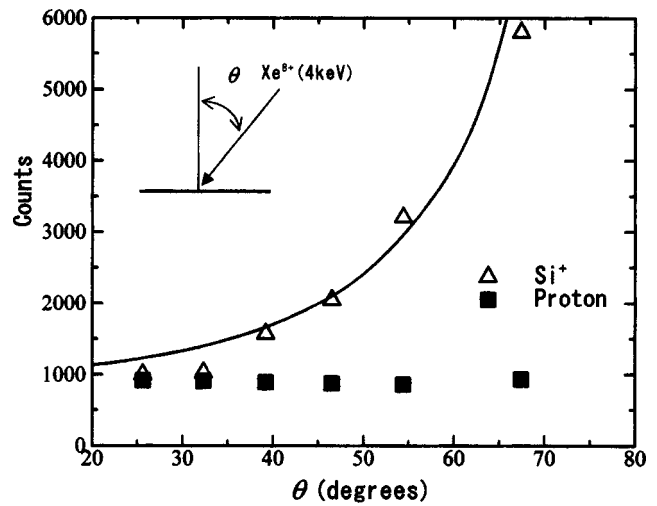


FIG. 3. Sputtering yields of proton and Si⁺ from a Si(100)2×1-H surface with 4 keV Xe⁸⁺ ions as a function of incident angle θ . The solid line shows $\cos^{-2} \theta$.

pact as a function of incident angle θ of the HCI. The Si⁺ ion yield drastically increased as θ increased, which is a specific feature to the kinetic sputtering.¹⁸ On the other hand, the proton yield did not depend on θ , again proving that the proton sputtering is not induced by a kinetic recoil effect that governs the kinetic sputtering.

All these experimental results observed for well-defined H-terminated Si surfaces are consistent with the proton sputtering model¹² proposed for untreated surfaces,^{9,10} which is schematically described in Fig. 4. The contour lines in the figure show electron distributions of H-Si-Si-H bonds.¹⁹ When an HCI approaches a surface, two or more electrons are transferred from a chemical bond on the surface to the HCI, resulting in mutual repulsion of two charged atoms in the bond. The repulsion causes the outer atom in the bond (which is hydrogen in the case of Fig. 4) to be ejected as an ion into vacuum. Considering that the ions in the bond are reneutralized within a finite time, the sputtering mechanism described earlier is expected to be effective for light elements like hydrogen. This is because a light ion moves quickly away from the bond area, and thus (1) is less likely to be reneutralized and (2) at the same time receives enough energy before the partner ion is reneutralized, which allows

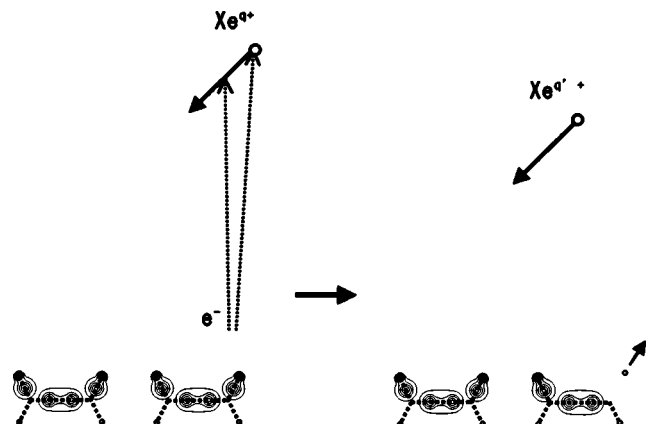


FIG. 4. Schematic diagram showing the potential sputtering of hydrogen with an HCI from the Si-H bond.

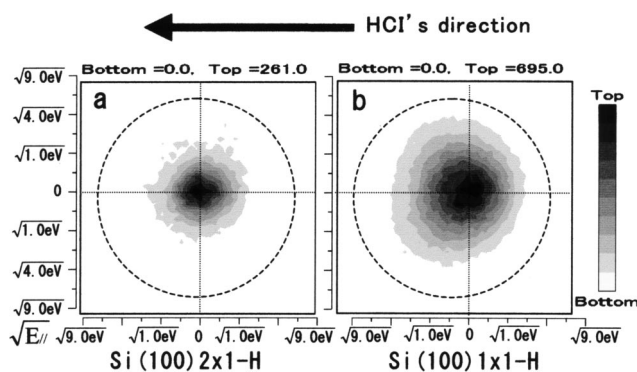


FIG. 5. Two-dimensional lateral \sqrt{E} distributions of sputtered protons from (a) the Si(100)2 \times 1-H and (b) the Si(100)1 \times 1-H surfaces with 3 keV Xe⁸⁺ ions. The incident angle of the HCl is 40°. The dashed circles show the active area of the detector.

overcoming an attractive force that may recover after the reneutralization of the partner ion. Whenever an electron is transferred from the bond to the HCl, it is a temporal molecular orbital and is shared by the bond and the HCl. The probability of the electron in the HCl orbit for a specific Si–H bond may be determined by the ratio of the phase space volume, which is $n^2:1$, where n is the principal quantum number of the electronic state of the transferred electron. Considering that $n \sim q$,⁶ the probability for the hydrogen to remain charged is proportional to q^2 . Crudely speaking, two-electron transfer from the same bond is a minimum requirement to induce effective ion emission, and the secondary ion yields induced with slow HCIs are expected to be proportional to q^4 or even stronger.

The absolute proton sputtering yields from the Si(100)2 \times 1-H, Si(100)3 \times 1-H, and Si(100)1 \times 1-H surfaces bombarded with 3 keV Xe⁸⁺ ions were $\sim 1.2 \times 10^{-4}$ /ion, $\sim 2.0 \times 10^{-4}$ /ion, and $\sim 1.3 \times 10^{-3}$ /ion, respectively. Thermal desorption spectroscopy measurements showed that the coverage of hydrogen for these surfaces was 1 monolayer (ML), 1.5 ML, and 2.0 ML, respectively, that is, the proton yield normalized per hydrogen surface density for the Si(100)1 \times 1-H surface was about five times larger than the other two. This large enhancement can be attributed to the fact that the Si(100)1 \times 1-H surface is atomically rough, while the Si(100)2 \times 1-H and Si(100)3 \times 1-H surfaces are atomically flat.²⁰ Such an atomically rough surface is formed because of a bond-breaking H-termination ($\text{H-Si}=\text{Si-H} + 2\text{H} \rightarrow 2\text{H-Si-H}$) and an etching reaction ($\text{H-Si-H} + 2\text{H} \rightarrow \text{SiH}_4$) during atomic hydrogen exposure at room temperature.²⁰ It is easy to imagine that an ion in the bond on an atomically rough surface is less likely to be reneutralized, as compared with that on an atomically flat surface. Further, reneutralization of Si⁺ ion may also be slower for a rough surface, leading to a prediction that the emission energy of proton for the Si(100)1 \times 1-H surface is higher than those for the Si(100)2 \times 1-H and Si(100)3 \times 1-H surfaces because the repulsive force between the proton and Si⁺ ion lasts

longer. Figures 5(a) and 5(b) show two-dimensional (2D) distribution¹⁴ of sputtered protons for Si(100)2 \times 1-H and Si(100)1 \times 1-H surfaces bombarded with 3 keV Xe⁸⁺, respectively. It is seen that the half width at half maxima for the Si(100)1 \times 1-H and Si(100)2 \times 1-H surfaces were ~ 1 and ~ 0.25 eV, respectively, which is at least qualitatively consistent with the above expectation. The 2D distributions consist only of a single peak at the center, which are not in accord with a naive expectation that the angular distribution of sputtered protons reflects the direction of the Si–H bond before sputtering and also is influenced by the Coulomb field of the HCl. It is also seen that the 2D distribution of protons for the Si(100)1 \times 1-H skewed slightly to the downstream side of the HCl, although that for the Si(100)2 \times 1-H was almost isotropic.

Summarizing, proton sputtering phenomena with slow HCIs were studied for three different well-defined H-terminated Si(100) surfaces. The proton sputtering yields for the Si(100)2 \times 1-H, Si(100)3 \times 1-H, and Si(100)1 \times 1-H surfaces bombarded with 3 keV Xe⁸⁺ ions were $\sim 1.2 \times 10^{-4}$ /ion, $\sim 2.0 \times 10^{-4}$ /ion, and $\sim 1.3 \times 10^{-3}$ /ion, respectively, and were proportional to q^γ ($\gamma \sim 5$). The yield, as well as the kinetic energy distribution of the sputtered protons, was consistent with the pair-wise potential sputtering model based on the over barrier model although the quantitative understanding on the angular distributions is left as an interesting future problem.

¹J. P. Briand, L. de Billy, P. Charles, S. Essabaa, P. Briand, R. Geller, J. P. Desclaux, S. Bliman, and C. Ristori, Phys. Rev. Lett. **65**, 159 (1990).

²H. Winter, Europhys. Lett. **18**, 207 (1992).

³H. Kurtz, K. Töglhofer, HP. Winter, F. Aumayr, and R. Mann, Phys. Rev. Lett. **69**, 1140 (1992).

⁴J. Das and R. Morgenstern, Phys. Rev. A **47**, R755 (1993).

⁵M. Grether, A. Spieler, R. Köhrbrück, and N. Stolterfort, Phys. Rev. A **52**, 426 (1995).

⁶J. Burgdörfer, P. Lerner, and F. W. Meyer, Phys. Rev. A **44**, 5674 (1991).

⁷S. Ninomiya, Y. Yamazaki, F. Koike, H. Masuda, T. Azuma, K. Komaki, K. Kuroki, and M. Sekiguchi, Phys. Rev. Lett. **78**, 4557 (1997).

⁸N. Kakutani, T. Azuma, Y. Yamazaki, K. Komaki, and K. Kuroki, Jpn. J. Appl. Phys. **34**, L580 (1995).

⁹N. Kakutani, T. Azuma, Y. Yamazaki, K. Komaki, and K. Kuroki, Nucl. Instrum. Methods Phys. Res. B **96**, 541 (1995).

¹⁰K. Kuroki, T. Takahira, Y. Tsuruta, N. Okabayashi, T. Azuma, K. Komaki, and Y. Yamazaki, Phys. Scr., T **80**, 557 (1999).

¹¹S. Della-Negra, J. Depauw, H. Joret, V. Le Beyec, and E. A. Schweikert, Phys. Rev. Lett. **60**, 948 (1988).

¹²J. Burgdörfer and Y. Yamazaki, Phys. Rev. A **54**, 4140 (1996).

¹³T. Neidhart, F. Pichler, F. Aumayr, H. P. Winter, M. Schmid, and P. Varga, Phys. Rev. Lett. **74**, 5280 (1995).

¹⁴N. Okabayashi, K. Kuroki, Y. Tsuruta, T. Azuma, K. Komaki, and Y. Yamazaki, Phys. Scr., T **80**, 555 (1999).

¹⁵K. Kuroki, H. Torii, K. Komaki, and Y. Yamazaki, Nucl. Instrum. Methods Phys. Res. B **193**, 804 (2002).

¹⁶N. Matsunami, Y. Yamamura, Y. Itikawa, N. Itoh, Y. Kazumata, S. Miyagawa, K. Morita, R. Shimizu, and H. Tawara, Atomic Data and Nuclear Data **31**, 1 (1984).

¹⁷S. T. De Zwart, T. Fried, D. O. Boerma, R. Hoekstra, A. G. Drentje, and A. L. Boers, Surf. Sci. **177**, L939 (1986).

¹⁸P. Sigmund, Phys. Rev. **184**, 383 (1969).

¹⁹C. J. Wu and E. A. Carter, Chem. Phys. Lett. **185**, 172 (1991).

²⁰J. J. Boland, Phys. Rev. Lett. **65**, 3325 (1990).